Coupled channels analysis of $^{19}F+^{12}C$ elastic and inelastic scattering using a cluster-folding interaction

H. Fujita
Daiichi College of Pharmaceutical Sciences, Fukuoka 815, Japan

N. Kato* and T. Sugimitsu
Department of Physics, Kyushu University, Fukuoka 812, Japan

Y. Sugiyama
Advanced Science Research Center, Japan Atomic Energy Research Institute, Tokai-mura, Ibaraki 319-11, Japan
(Received 23 December 1993; revised manuscript received 22 June 1994)

Angular distributions for elastic and inelastic scattering of the $^{19}F+^{12}C$ system leading to the $\frac{1}{2}^+$ (g.s.), $\frac{5}{2}^+$ (0.197 MeV), $\frac{3}{2}^+$ (1.554 MeV), and $\frac{9}{2}^+$ (2.780 MeV) states in ^{19}F were calculated with a coupled channels (CC) method using cluster folding (CF) interactions based on a $^{16}O+t+^{12}C$ three-body model at $E_L(^{12}C)$=30–60 MeV. The calculations reproduce well the experimental angular distributions for the elastic and inelastic scattering to the $\frac{5}{2}^+$ and $\frac{3}{2}^+$ states at all energies, although for the inelastic scattering to the $\frac{5}{2}^+$ and $\frac{3}{2}^+$ states the phases of the calculated angular distributions seem to be shifted slightly backward from the experimental ones. The calculations are compared with the CC calculations using Woods-Saxon interaction in order to investigate the effect of the shape of the interaction.

PACS number(s): 25.70.Bc

I. INTRODUCTION

In the $^{19}F+^{12}C$ system, it has been found [1,2] that the phases of the angular distributions of the differential cross sections for inelastic scattering leading to the lowest $\frac{5}{2}^+$ (0.197 MeV) and $\frac{3}{2}^+$ (1.554 MeV) states in ^{19}F at $E_L(^{12}C)$=30–60 MeV cannot be reproduced by distorted-wave Born approximation (DWBA) and coupled channels (CC) calculations with usual macroscopic rotational form factors. These states are interpreted as members of the ground-state ($K^\pi = \frac{1}{2}^+$) rotational band. They are expected, therefore, to be populated strongly by the $L = 2$ transition and to show a phase relation predicted by the usual DWBA and CC calculations with macroscopic form factors, in which the oscillation for inelastic scattering is almost out of phase with the one for elastic scattering. However, it was found that the experimental angular distributions for inelastic scattering to the lowest $\frac{5}{2}^+$ and $\frac{3}{2}^+$ states are shifted forward with respect to the predicted ones. The most remarkable discrepancy can be seen in the data at 40 MeV, where the phases of the angular distribution for inelastic scattering to the $\frac{5}{2}^+$ and $\frac{3}{2}^+$ states are almost in phase with the experimental one for elastic scattering and out of phase with the predicted ones including only the $L = 2$ coupling as shown in Figs. 2 and 3 of Ref. [1], although inclusion of the $L = 4$ coupling improves the fit of the calculations to the data as shown by the dashed lines in Fig. 10 of Ref. [2]. In addition, it should be noted that the angular distribution for inelastic scattering to the 2^+ (4.439 MeV) state of ^{12}C is almost out of phase with that for elastic scattering and reproduced by a usual CC calculation as shown in Fig. 6 of Ref. [2]. A recent study [2] has shown that the CC calculations including a repulsive spin-orbit (SO) force reproduce well the above angular distributions at all the energies. However, the origin of the phenomenological SO force introduced is not clear. As mentioned in Sec. II, the theoretical SO force expected from the folding model is attractive and about one order of magnitude smaller than the SO force of Ref. [2]. The phenomenological SO force, therefore, could not be simply considered to be a bare SO interaction, but may reflect various effects ignored in the above CC calculations. One of the possible origins of the present phase anomaly is due to the structure of the ^{19}F nucleus.

In the past decade, CC and continuum-discretized coupled channels (CDCC) studies [3–8] using cluster-folding (CF) and double-folding (DF) interactions have been performed for scattering by polarized or unpolarized light-heavy beams (^6Li, ^7Li, ^9Be, ^{12}C, and so on) which have well-developed cluster structures and have provided a successful understanding of the experimental data of both cross sections and spin observables. These CC and CDCC studies have clearly shown that virtual excitations of the incident light-heavy ions to bound states and/or continuum states produce effective interactions, i.e., central and spin-dependent ones. As for the case of ^{19}F, Ohkubo and Kamimura [9] have applied the CC method using a CF interaction to the elastic scattering of ^{19}F on ^{28}Si at $E_L = 60$ MeV in order to investigate the dynami-

*Deceased.

cally induced SO interaction in the ^{19}F+^{28}Si system. The low-lying positive parity states of ^{19}F are considered to have a cluster structure of t+^{16}O configuration [10,11]. In this study [9], however, inelastic scattering was not described at all.

In the present work, we have investigated how phases of the angular distributions for elastic and inelastic scattering are affected by the CC calculations with the CF or DF interaction for the ^{19}F+^{12}C system. We have employed a CF interaction based on the ^{16}O+t+^{12}C three-body model, for simplicity, and performed the analyses of the elastic and inelastic scattering for the ^{19}F+^{12}C system at $E_L(^{12}\mathrm{C})$=30.01, 40.32, 50.04, and 60.06 MeV, taking into account the coupling of the four low-lying positive parity states of ^{19}F, i.e., the $\frac{1}{2}^+$ (g.s.), $\frac{5}{2}^+$ (0.197 MeV), $\frac{3}{2}^+$ (1.554 MeV), and $\frac{9}{2}^+$ (2.780 MeV) states.

II. PROCEDURE OF THE ANALYSIS

The theoretical framework of the coupled channels (CC) method using the cluster-folding (CF) interaction based on the three-body model as well as its applications to light-heavy ion scattering is given in many papers [3,4,6,7]. The analyses were performed according to the following procedure. The low-lying positive parity states of ^{19}F were assumed to be constructed from a t+^{16}O cluster. In the CF model, the diagonal and nondiagonal ^{19}F+^{12}C interactions are constructed by folding the existing t+^{12}C and ^{16}O+^{12}C optical potentials as

$$V_{ij}(\mathbf{R}) = \langle \psi_i(\mathbf{r}) | V_t(\mathbf{R} + \tfrac{16}{19}\mathbf{r}) + V_{\mathrm{O}}(\mathbf{R} - \tfrac{3}{19}\mathbf{r}) | \psi_j(\mathbf{r}) \rangle \ .$$

Here V_t and V_{O} are the t+^{12}C and ^{16}O+^{12}C optical potentials evaluated at $E_L(t) \approx \frac{3}{19}E_L(^{19}\mathrm{F})$ and $E_L(^{16}\mathrm{O}) \approx \frac{16}{19}E_L(^{19}\mathrm{F})$, respectively, while ψ_i (ψ_j) represents the wave function for the t+^{16}O relative motion in the ith (jth) state of ^{19}F. The wave functions of the ground and excited states of ^{19}F were constructed according to the t+^{16}O cluster model given by Buck and Pilt [10], in the present work. This model treats the low-lying positive parity states of ^{19}F as eigenstates of a local t+^{16}O potential and reproduces well the observed properties of these states [10]. The low-lying negative parity states, e.g., $\frac{1}{2}^-$ (0.110 MeV), $\frac{5}{2}^-$ (1.346 MeV), and $\frac{3}{2}^-$ (1.459 MeV) states, can be considered to be α+^{15}N cluster states [10,11] and then cannot be treated within the framework of the ^{16}O+t+^{12}C three-body model. In the present analyses, therefore, these low-lying negative parity states were neglected, although significant β_3 values have been obtained for the $\frac{5}{2}^-$ state from the DWBA analyses of the light ion inelastic data [12–15]. The calculations of the wave functions ψ_i and the interactions V_{ij} were carried out by using a computer code [16] which was developed for construction of the wave functions and the interactions used in the CDCC calculations for ^{6,7}Li by Kamimura and collaborators and modified for ^{19}F by Kamimura.

The optical potentials for the t+^{12}C system at $E_L(t)$ = 7.5, 10.1, 12.5, and 15.0 MeV should be used in the present analyses, corresponding to the incident energies of 30.01, 40.32, 50.04, and 60.06 MeV, respectively, of ^{12}C for the ^{19}F+^{12}C system. Although several sets of optical potentials for the t+^{12}C system are available [17–20] in the present energy region, we adopted the optical potentials determined by Fick *et al.* at $E_L(t)$ = 8.97 and 10.97 MeV [20] (abbreviated to the 9 and 11 MeV potentials hereafter). These potentials were deduced from both differential cross section and vector analyzing powers with a polarized triton beam, while the others [17–19] were determined with an unpolarized triton beam.

As for the optical potentials for the ^{16}O+^{12}C system, those at $E_L(^{16}\mathrm{O})$=40.0, 53.8, 66.7, and 80.1 MeV are needed. The parameters of the four ^{16}O+^{12}C optical potentials adopted in the present analyses are given in Table I. The potential set A was determined at $E_L(^{16}\mathrm{O})$=42 MeV by Voos, von Örtzen, and Bock [21] and used in the analysis of the data at $E_L(^{12}\mathrm{C})$=30.01 MeV for the ^{19}F+^{12}C system. Set B has been determined so as to reproduce the differential cross sections at forward angles ($\theta_{\mathrm{c.m.}} < 60°$) for the elastic scattering at $E_L(^{16}\mathrm{O})$=52.7 and 55.1 MeV. These data have been obtained by using the Kyushu University Tandem Accelerator in order to study the spin alignment of the 3^- (6.13 MeV) state of ^{16}O from ^{16}O+^{12}C inelastic scattering [22]. The parameters of the potential were searched automatically with the optical model code SEARCH [23] by starting from the potential [24] which was determined by Charles *et al.* to reproduce the forward angle cross sections around $E_L(^{16}\mathrm{O})$=52.5 MeV. Figure 1 shows the results of the

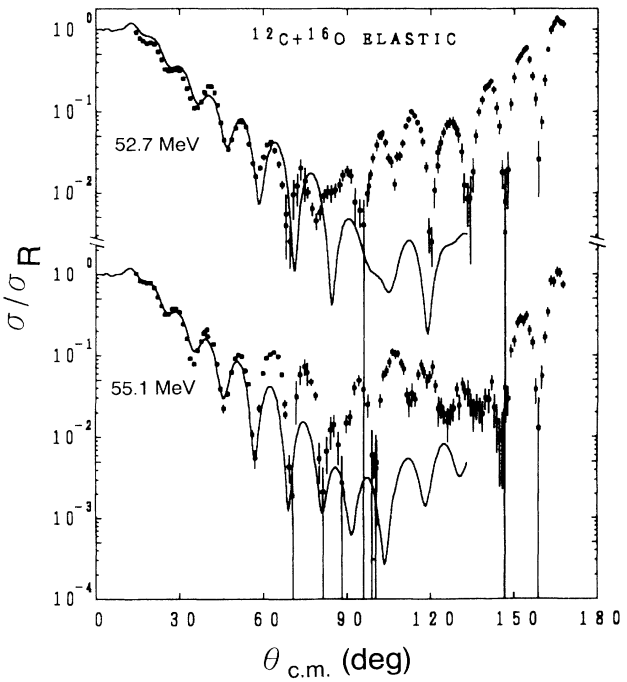

FIG. 1. Optical model calculations for the ^{16}O+^{12}C system using the potential set B in Table I at $E_L(^{16}\mathrm{O})$=52.7 and 55.1 MeV. The experimental data were obtained by using the Kyushu University Tandem Accelerator. For details, see text.

TABLE I. Parameters of ^{16}O+^{12}C optical potentials.[a]

Set	$E_L(^{16}O)$ (MeV)	V (MeV)	r_R (fm)	a_R (fm)	W (MeV)	r_I (fm)	a_I (fm)	r_C (fm)
A[b]	42	25	1.22	0.49	139.0	0.75	0.38	1.4
B[c]	52.7,55.1	90.0	1.16	0.49	18.5	0.90	0.30	1.4
C[d]	65	100	1.18	0.45	30.0	1.25	0.18	1.45
D[d]	80	100	1.09	0.54	30.0	1.21	0.27	1.45

[a]Wood-Saxon form is assumed. The radii are defined as $R_{R,I,C} = r_{R,I,C}(A_p^{1/3} + A_t^{1/3})$.
[b]Reference [21].
[c]Determined in the present work.
[d]Reference [25].

optical model calculation using the potential set B with the experimental data. The potential set B improves the fit of the CC calculation to the data compared with the potential by Charles *et al.* and was used in the analysis at $E_L(^{12}C)$= 40.32 MeV for the ^{19}F+^{12}C system. Sets C and D have been determined at $E_L(^{16}O)$=65 and 80 MeV, respectively, by Gutbrod *et al.* [25] and used in the analyses at $E_L(^{12}C)$= 50.04 and 60.06 MeV, respectively.

The CC calculations were performed with the diagonal ($i = j$) and coupling ($i \neq j$) potentials V_{ij} obtained above. In the standard CC method with a CF interaction, once a certain set of potential parameters for V_t and V_O are chosen, there is no adjustable parameter in the calculations. For ^{6}Li-nucleus scattering, additional renormalization factors for the real and imaginary parts of CF model interactions have been introduced in order to get a reasonable fit to the data [26–28]. In the present system, however, these renormalization factors were not needed. The angular distributions of the differential cross sections of the elastic and inelastic scattering for the ^{19}F+^{12}C system leading to the $\frac{1}{2}^+$, $\frac{5}{2}^+$, $\frac{3}{2}^+$, and $\frac{9}{2}^+$ states in ^{19}F were obtained. The coupling scheme is illustrated in Fig. 2. Angular momentum transfers up to

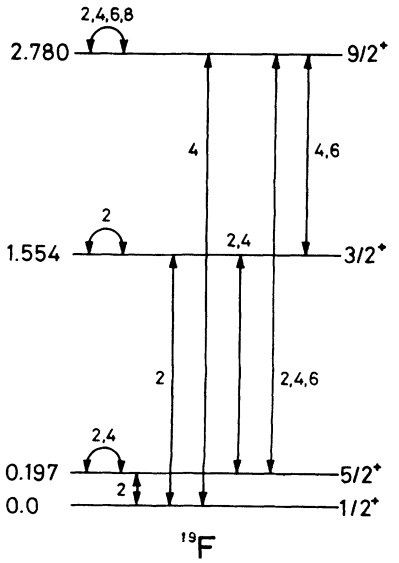

FIG. 2. Full coupling scheme for the calculations. The numbers alongside each arrow represent the values of transferred angular momenta.

$8\hbar$ were taken into account in the calculations. The calculations were carried out using a coupled channels code [29] developed by Kamimura and collaborators.

In the present analyses the folding SO interaction and the Coulomb excitation were not included for simplicity. The cluster-folding SO potential for the ground state is obtained by calculating Eqs. (3) and (4) of Ref. [30]. The values obtained by using the 9 and 11 MeV potentials of Ref. [20] are −2.3 and −4.4 keV, respectively, at the strong absorption radius $R_s \approx 1.5 \times (19^{1/3} + 12^{1/3}) = 7.4$ fm. The absolute values are about one order of magnitude smaller than that (26.5 keV) of the empirical SO potential introduced in Ref. [2], and the signs are opposite the empirical one. In the present case, therefore, the influence of the cluster-folding SO potential is expected to be small. The CC calculations including a Coulomb excitation were performed among the $\frac{1}{2}^+$, $\frac{5}{2}^+$, and $\frac{3}{2}^+$ states. The influence of the Coulomb excitation was small on both the magnitude and phase of the cross sections in the present regions of energy and angle, and the conclusions obtained by the present study were not altered by the absence of the Coulomb excitation at least within the three-channel calculations. The main purpose of the present paper is to examine the effect of the shape of the nuclear interaction. We have ignored the Coulomb excitation in the present analyses in order to avoid an increase of computing time by including the $\frac{9}{2}^+$ state.

III. RESULTS AND DISCUSSIONS

A. Results of full CC calculations

The results of the full CC calculations are shown in Figs. 3–6. The result (dashed lines) obtained by using the 9 MeV potential of Ref. [20] as the t+^{12}C optical potential and that (solid lines) by using the 11 MeV potential are in good agreement with each other at all energies. The experimental angular distributions for elastic scattering are reproduced well by the calculations at all energies except minor discrepancies. These discrepancies might be eliminated if more suitable potentials are used as V_t or V_O. For inelastic scattering to the $\frac{5}{2}^+$ and $\frac{3}{2}^+$ states (only the $\frac{5}{2}^+$ state for the 30 MeV data), the magnitude and shape of the angular distributions are reproduced fairly well by the calculations, but the phases

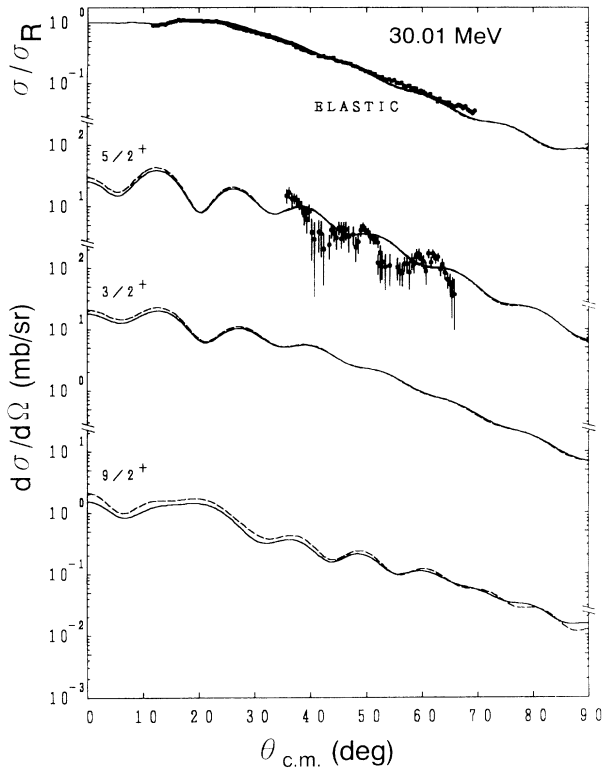

FIG. 3. Results of full CC calculations at $E_L(^{12}\mathrm{C})$=30.01 MeV. The dashed and solid lines show the results using the t+^{12}C optical potentials determined at $E_L(t)$ = 8.97 and 10.97 MeV, respectively.

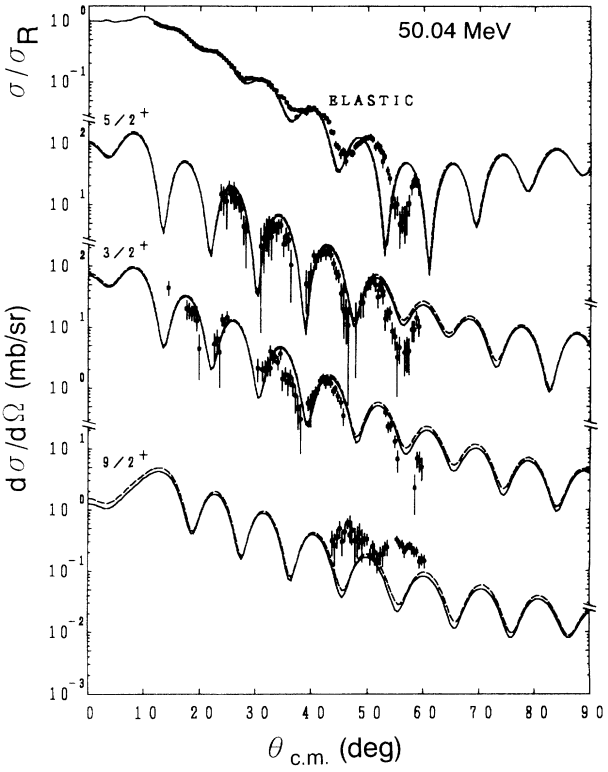

FIG. 5. Same as Fig. 3, but at $E_L(^{12}\mathrm{C})$=50.04 MeV.

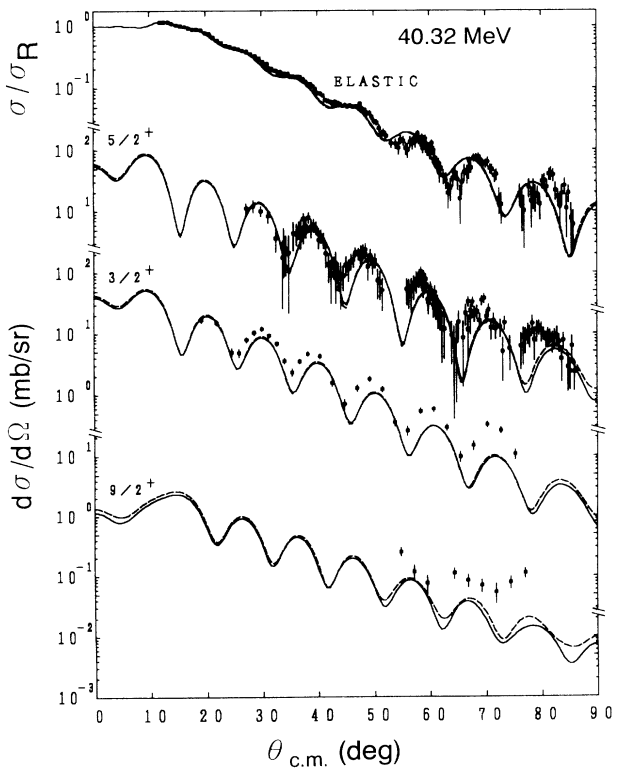

FIG. 4. Same as Fig. 3, but at $E_L(^{12}\mathrm{C})$=40.32 MeV.

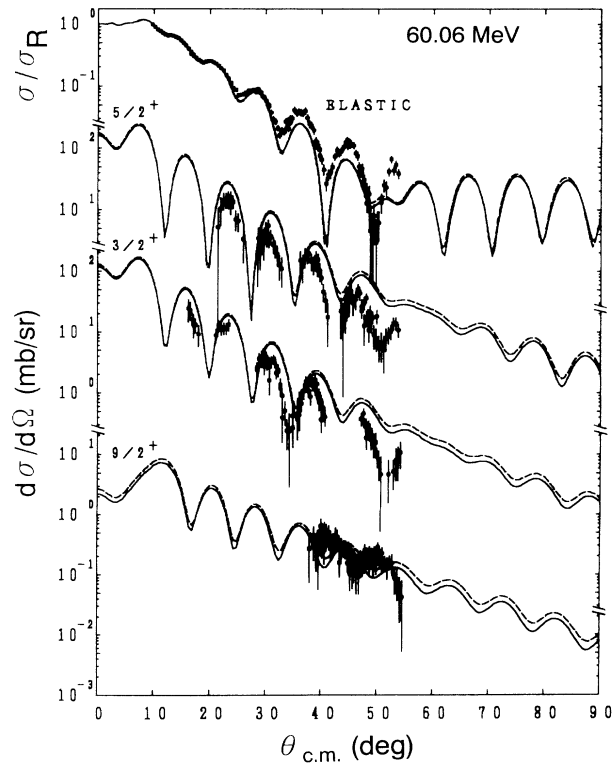

FIG. 6. Same as Fig. 3, but at $E_L(^{12}\mathrm{C})$=60.06 MeV.

seem to be shifted slightly forward from the calculations, as in the analyses [1,2] with a macroscopic model, at all the energies.

All the $^{16}O+^{12}C$ optical potentials used here do not reproduce the backward angle cross sections for the $^{16}O+^{12}C$ elastic scattering as shown in Fig. 1 for the potential set B. It is considered [31] that the backward rise of the differential cross sections in the elastic scattering for this system is due to elastic transfer of an α particle. In the present analyses, however, we treat only the forward angle data and the influence of elastic transfer has been considered [32] to be small at forward angles. All the potentials given in Table I have been obtained so as to reproduce only the forward angle data. These potentials may not be "bare" $^{16}O+^{12}C$ optical ones. We think, however, it is worthwhile that the CC calculations using the potentials in Table I give reasonable fits to the data.

B. Coupling effects of individual channels

In order to investigate how the CC calculations, taking account of the effects of the structure of ^{19}F, affect the cross sections for elastic and inelastic scattering, we first examined the coupling effects of the individual channels. Five types of CC calculations were compared; the ^{19}F states included in the five calculations were (i) the $\frac{1}{2}^+$ (ground) state only, (ii) the $\frac{1}{2}^+$ and $\frac{5}{2}^+$ states, (iii) the $\frac{1}{2}^+$ and $\frac{3}{2}^+$ states, (iv) $\frac{1}{2}^+$, $\frac{5}{2}^+$, and $\frac{3}{2}^+$ states, and (v) the $\frac{1}{2}^+$, $\frac{5}{2}^+$, $\frac{3}{2}^+$, and $\frac{9}{2}^+$ states. The results at 40.32 MeV are shown in Fig. 7. The 11 MeV potential of Ref. [20] and the potential set B in Table I were used as V_t and V_O, respectively. The phases of the angular distributions for the elastic scattering by the (i) one-channel, (ii) two-channel ($\frac{1}{2}^+$-$\frac{5}{2}^+$), and (iii) two-channel ($\frac{1}{2}^+$-$\frac{3}{2}^+$) calculations are shifted slightly forward from the one by the (v) four-channel calculation (namely, the full CC calculation), while for inelastic scattering the phases by both two-channel calculations are shifted very slightly backward from the full CC calculation and the magnitudes increase a little. The results of the (iv) three-channel ($\frac{1}{2}^+$-$\frac{5}{2}^+$-$\frac{3}{2}^+$) calculation are in good agreement with the ones of the (v) full CC calculation except for the $\frac{5}{2}^+$ state. The long-dashed line (the three-channel calculation) for the $\frac{5}{2}^+$ state deviates a little upward from the solid line (the full CC calculation). Namely, the role of the $\frac{9}{2}^+$ state is very small for the ground and $\frac{3}{2}^+$ states, and even for the $\frac{5}{2}^+$ state only the magnitude of the angular distribution is slightly affected by including the $\frac{9}{2}^+$ state, but the phase is hardly affected.

Figure 8 shows the results of the one-channel calculations, namely, the usual potential scattering calculations by the use of the CF interactions, and the ones of the full CC calculations for elastic scattering at the four energies. The 11 MeV potential was used as V_t. The dotted and solid lines indicate the results of the one-channel calculations and the full CC ones, respectively, without the

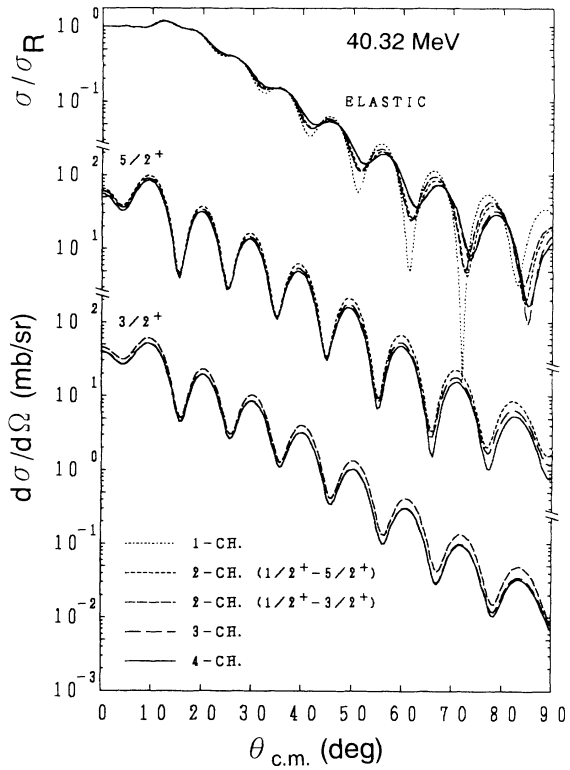

FIG. 7. Effect of channel coupling at $E_L(^{12}C)$=40.32 MeV. For details, see text.

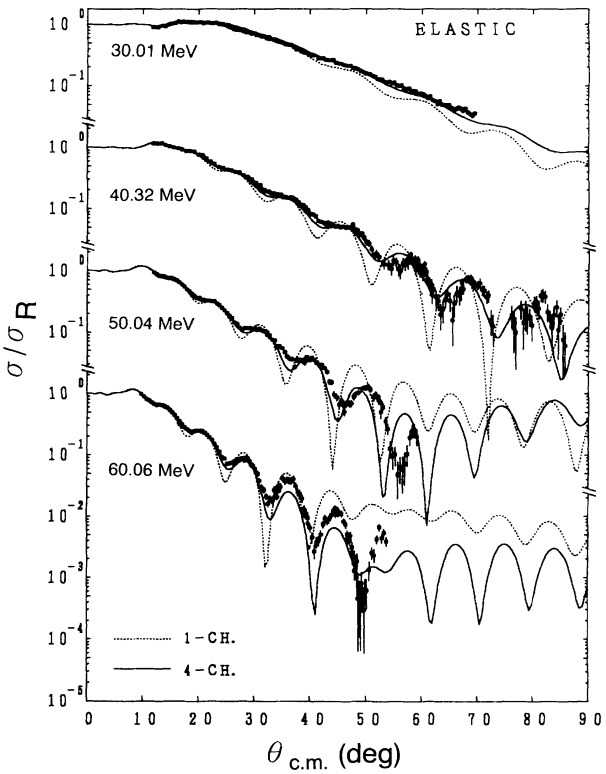

FIG. 8. Results of the CC calculations for the elastic scattering at the four energies. The dotted lines show the results of the one-channel calculations, namely, usual potential scattering calculations, and the solid lines show those of the four-channel CC calculations.

additional renormalization factors. There are remarkable differences between the one-channel calculations and the full CC ones, and the experimental data are well reproduced by the full CC calculations at all energies. As mentioned before, the phases of the angular distributions by the full CC calculations are shifted slightly backward from the ones by the one-channel calculations. If we try to fit reasonably the results of the full CC calculations by the one-channel calculations with the CF interactions multiplied by the renormalization factors, N_R for the real part and N_I for the imaginary part, the following values are needed: $(N_R, N_I) = (0.68, 3.5)$, $(0.72, 3.0)$, $(0.82, 2.4)$, and $(0.85, 1.8)$ at $E_L(^{12}\mathrm{C})$=30.01, 40.32, 50.04, and 60.06 MeV, respectively. Two extreme cases of dynamical polarization (DP) potentials have been well investigated [6,7,33]: One is the usual DP potential induced by excitation of collective modes [34,35], having a very small real part ($\Delta V \simeq 0$) and a sizable and absorptive imaginary part ($\Delta W < 0$), and the other is that induced by coupling to the breakup channels [5–7], having a repulsive real part ($\Delta V > 0$) and a negligible small imaginary part ($\Delta W \simeq 0$). The present case, in which the real DP potentials are repulsive ($\Delta V > 0$) and the imaginary parts are strongly absorptive ($\Delta W < 0$), is different from the above two cases. Although further investigation is necessary in order to understand the meaning of the present DP potentials, it should be noted that the present DP potentials are caused at least partly by the $L = 4$ coupling between the $\frac{5}{2}^+$ and $\frac{3}{2}^+$ states as mentioned below.

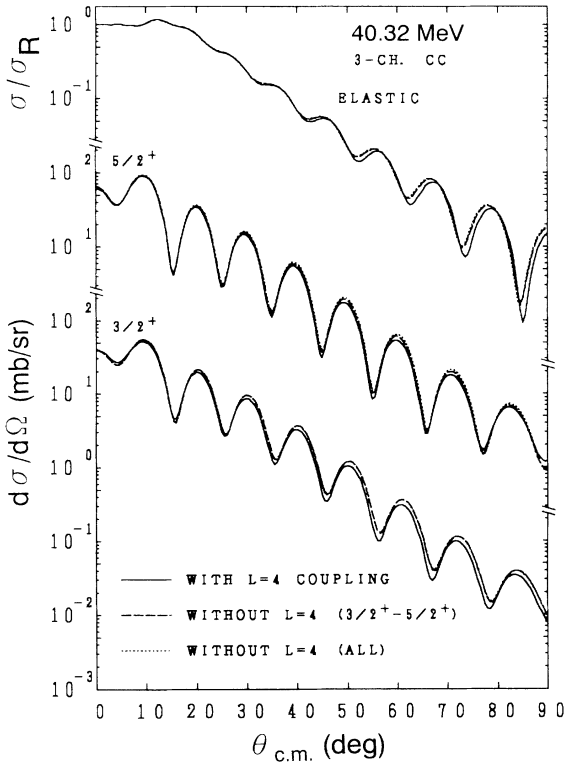

FIG. 9. Effect of the coupling between the $\frac{5}{2}^+$ and $\frac{3}{2}^+$ states at $E_L(^{12}\mathrm{C})$=40.32 MeV. The solid lines indicate the result of the three-channel CC calculation with both the $L = 2$ and 4 couplings between the $\frac{5}{2}^+$ and $\frac{3}{2}^+$ states. The dashed and dotted lines indicate the results without the $L = 4$ coupling between the $\frac{5}{2}^+$ and $\frac{3}{2}^+$ states and without all the $L = 4$ couplings (i.e., the $L = 4$ coupling between the $\frac{5}{2}^+$ and $\frac{3}{2}^+$ states and the $L = 4$ reorientation coupling of the $\frac{5}{2}^+$ state), respectively.

The role of the coupling between the $\frac{5}{2}^+$ and $\frac{3}{2}^+$ states was examined in order to clear up the difference of the phases between the two- and three-channel calculations, because the effect of including the $\frac{9}{2}^+$ state is small, especially on the phase. The $L = 2$ and 4 couplings can exist between the $\frac{5}{2}^+$ and $\frac{3}{2}^+$ states. Figure 9 shows the results of the three-channel calculations at 40.32 MeV. The used potentials are the same as in Fig. 7. The solid lines indicate the result with both the $L = 2$ and 4 couplings. The dashed and dotted lines indicate the results without the $L = 4$ coupling between the $\frac{5}{2}^+$ and $\frac{3}{2}^+$ states and without all the $L = 4$ couplings, respectively. As shown in Fig. 9, if the $L = 4$ coupling between the $\frac{5}{2}^+$ and $\frac{3}{2}^+$ states is excluded, the peaks and valleys of the angular distribution for the elastic scattering are shifted forward and those for the inelastic one are very slightly shifted backward. Thus the $L = 4$ coupling between the $\frac{5}{2}^+$ and $\frac{3}{2}^+$ states improves the fit, particularly for elastic scattering, and then contributes the DP potentials as mentioned above. On the other hand, the $L = 2$ coupling between the $\frac{5}{2}^+$ and $\frac{3}{2}^+$ states scarcely affected the phase.

C. Effects of the structure of ^{19}F

Next we investigated how the shape of the interaction affects the differential cross sections. Figure 10 shows the diagonal form factor of the ground state at 40.32 MeV with the 11 MeV potential of Ref. [20] as V_t and the potential set B in Table I as V_{O}. The form factors obtained by the CF model are given as the sum of the interaction between core cluster (^{16}O) and partner nuclei (^{12}C) and the one between the valence cluster (t) and partner one (^{12}C). In the cluster model, the ratio of the distance of the ^{16}O core cluster from the center of mass of ^{19}F to the one of the t valence cluster from the center of mass of ^{19}F is $\frac{3}{16}$. Therefore, in the surface region (i.e., in the vicinity of the strong absorption radius $R_s \approx 7.4$ fm), the interactions have two components of different slopes, and in the region of larger distances only the t component contributes.

We examined the role of the shape of the interaction by comparing the CC calculation using the CF interaction with that using a Woods-Saxon- (WS-) type optical potential. We compared the results of the four-channel calculations. The result at 40.32 MeV is shown in Fig. 11. The dotted lines indicate the result of the four-channel calculation with the WS optical potential which was obtained so as to fit the angular distribution for the elastic scattering obtained by the four-channel calculation with the CF interaction. The 40 MeV potential not including the SO force in Table 2 of Ref. [2] was used as the starting potential. The CC calculation was performed by using

a heavy ion version [36] of the CC code JUPITOR-1 [37]. The deformation parameters $\beta_2 = 0.22$ and $\beta_4 = 0.06$ were used, and the $L = 2$ and 4 couplings were taken into account according to Eqs. (15) and (16) of Ref. [38]. The Coulomb excitation was not included. As shown in Fig. 11, the CC calculation with the WS potential reproduces very well the angular distributions from the CC calculations with the CF interaction except for discrepancy for the $\frac{9}{2}^+$ state. Similar results were obtained also at other three energies. The dashed lines in Fig. 11 indicate the result of the four-channel calculation using the CF interaction without the $L = 6$ and 8 couplings, which can be compared directly with the calculation by the use of JUPITOR-1 taking account of the multipole transitions up to 4. As seen in Fig. 11, the effect of the $L = 6$ and 8 couplings is small even for the $\frac{9}{2}^+$ state. Further, we examined the role of the $L = 4$ coupling in the CC calculation with the WS potential. In Fig. 12 the solid and dashed lines indicate the results of the four- and three-channel calculations, respectively, including the $L = 2$ and 4 couplings at 40.32 MeV. The calculations were performed using the same WS potential and the same deformation parameters as used in Fig. 11. The hexadecapole deformation was included according to Eqs. (15) and (16) of Ref. [38] even when the $L = 4$ coupling was not taken into account in the CC calculations. The result of the three-channel calculation for the $\frac{1}{2}^+$, $\frac{5}{2}^+$ and $\frac{3}{2}^+$ states is in good agreement with that of the four-channel one. This situation is the same as the case of the three- and

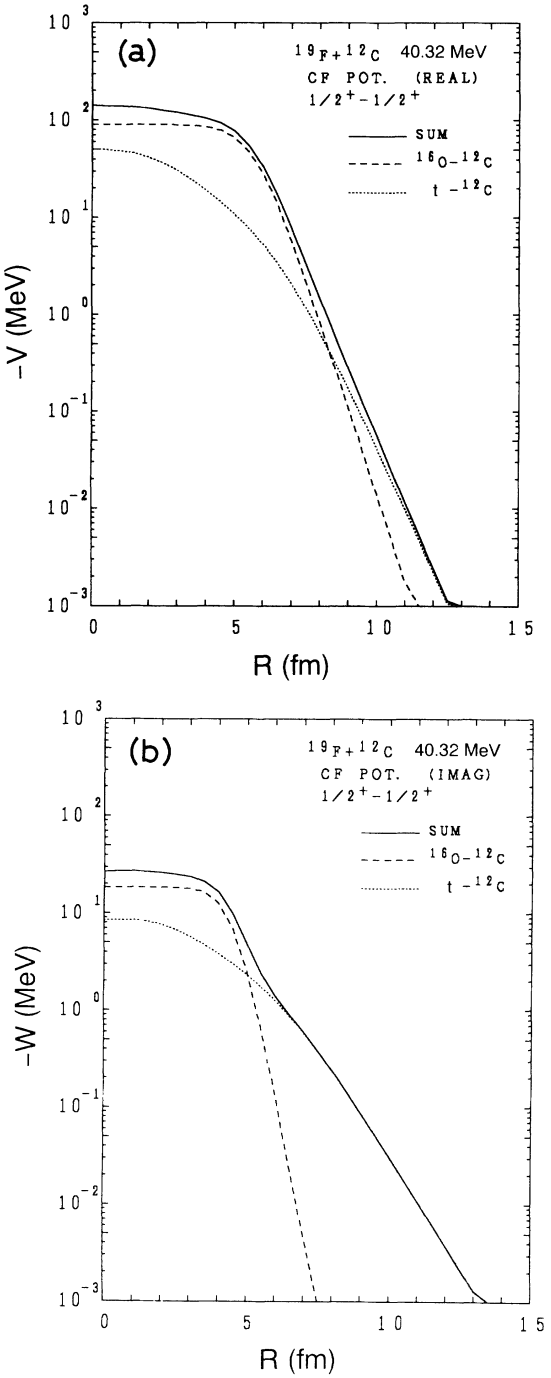

FIG. 10. Cluster-folding form factors for 40.32 MeV obtained using set B in Table I and the 11 MeV potential of Ref. [20] as V_0 and V_t, respectively. The (a) real and (b) imaginary parts of the diagonal potential for the ground state are shown. The dotted and dashed lines indicate the t+^{12}C and ^{16}O+^{12}C components, respectively. The solid lines indicate the total folding interactions, i.e., the sum of the two components.

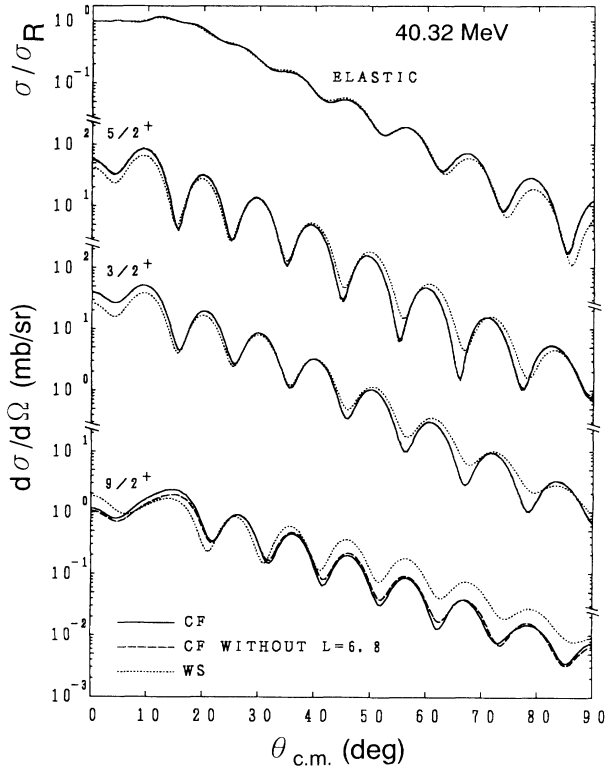

FIG. 11. Comparison of the result of the four-channel calculation using the Woods-Saxon interaction (dotted lines) with that using the cluster-folding interaction (solid lines) at 40.32 MeV. For details, see text. The dashed lines indicate the result using the cluster-folding interaction without the $L = 6$ and 8 couplings. The parameters of the used Woods-Saxon potential are as follows: $V = 19.63$ MeV, $r_R = 1.277$ fm, $a_R = 0.620$ fm, $W = 4.41$ MeV, $r_I = 1.424$ fm, $a_I = 0.620$ fm, and $r_C = 1.2$ fm.

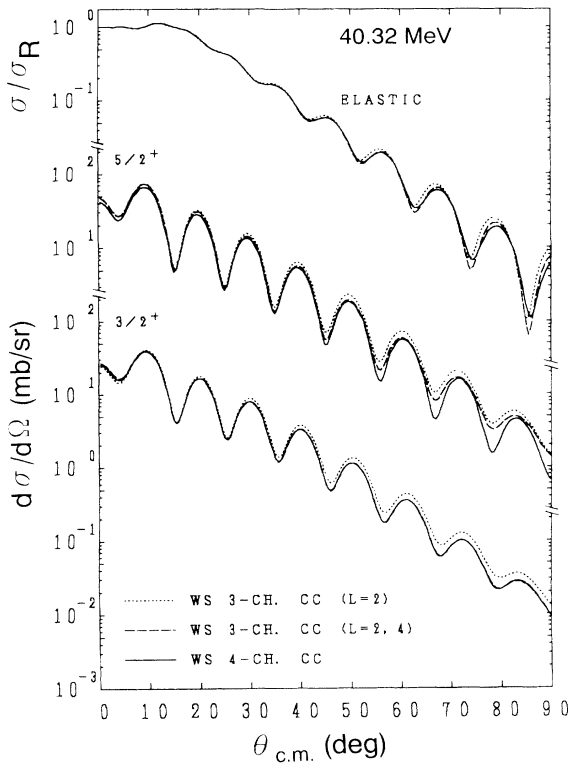

FIG. 12. Effect of the $L = 4$ coupling in the CC calculation using the Woods-Saxon potential. The dotted and dashed lines indicate the results of the three-channel calculations with the $L = 2$ coupling and with the $L = 2$ and 4 couplings, respectively. The solid lines show the result of the four-channel calculation with the $L = 2$ and 4 couplings.

four-channel calculations with the CF interaction shown in Fig. 7. The dotted lines in Fig. 12 indicate the result of the three-channel calculation with the WS interaction including only the $L = 2$ coupling. The dotted line for the elastic scattering is shifted slightly forward from the dashed and solid lines, whereas for the inelastic scattering changes of the phases are not evident, though the upward deviations are seen. This situation is also very similar to the case of using the CF interaction as shown in Fig. 9.

Earlier studies [1,2] have found for the so-called phase anomaly for the ^{19}F+^{12}C system that the angular distributions for elastic and inelastic scattering leading to the $\frac{5}{2}^+$ and $\frac{3}{2}^+$ states cannot be reproduced by the CC calculations with the WS potentials and the rotational form factors, but are reproduced by the CC calculations including the additional SO forces. Therefore it is concluded from the fact described above that the shape of the CF interaction has no recognizable effect on the present phase problem.

IV. SUMMARY AND CONCLUSIONS

Coupled channels calculations using cluster-folding interactions were performed based on the ^{16}O+t+^{12}C three-body model for the ^{19}F+^{12}C system, considering the low-lying positive parity states of ^{19}F as the cluster ones of the t+^{16}O configuration. The angular distributions of the differential cross sections for elastic scattering are reproduced well by the calculation at all the energies. For inelastic scattering to the $\frac{5}{2}^+$ and $\frac{3}{2}^+$ states, the angular distributions are reproduced fairly well by the calculations, although the phases of the calculated angular distributions seem to be shifted slightly backward from the experimental ones.

In order to investigate how the CC calculations with the CF interaction, taking account of the effect of the structure of ^{19}F, affect the angular distributions for elastic and inelastic scattering, various effects were examined. First, the coupling effects of the individual channels were examined. The results are summarized as follows. The full CC calculations reproduce the data for elastic scattering at all the energies, while the one-channel calculations do not reproduce the data. The effect of the $\frac{9}{2}^+$ state is small for both elastic and inelastic scattering to the $\frac{5}{2}^+$ and $\frac{3}{2}^+$ states. The $L = 4$ coupling between the $\frac{5}{2}^+$ and $\frac{3}{2}^+$ states is important for reproducing the phases of the angular distributions for elastic scattering. The phases of the angular distributions for inelastic scattering were little influenced by the couplings examined in this work. Next we examined the effect of the shape of the interaction by comparing with the CC calculations using the Woods-Saxon (WS) interactions. As the result, the CC calculations including the $L = 4$ coupling with the appropriate WS interaction reproduced very well the angular distributions obtained with the CF interaction. Further, the effect of the $L = 4$ coupling between the $\frac{5}{2}^+$ and $\frac{3}{2}^+$ states was similarly important for the CC calculations with the WS interaction. These results show that the shape of the CF interaction can be replaced by the Woods-Saxon form in the present case.

ACKNOWLEDGMENTS

The authors would like to express their sincere thanks to Professor M. Kamimura for his kind guidance and helpful suggestions to the coupled channels analysis using the cluster-folding interaction and for providing and modifying the program codes with which we could evaluate the wave functions of ^{19}F and the cluster-folding interactions (of central parts) and perform the coupled channels calculations. The authors would like to thank Professor S. Morinobu for his useful discussions and encouragement. The numerical calculations were carried out at the Computer Center of Kyushu University.

[1] T. Tachikawa, N. Kato, H. Fujita, K. Kimura, T. Sugimitsu, K. Morita, K. Anai, T. Inoue, Y. Nakajima, M. H. Tanaka, and S. Kubono, Phys. Lett. **139B**, 267 (1984).
[2] T. Tachikawa, N. Kato, H. Fujita, K. Anai, H. Inoue, T. Sugimitsu, K. Kimura, Y. Nakajima, K. Morita, S. Kubono, and M. H. Tanaka, Nucl. Phys. **A484**, 125 (1988).
[3] H. Nishioka, R. C. Johnson, J. A. Tostevin, and K.-I. Kubo, Phys. Rev. Lett. **48**, 1795 (1982); H. Nishioka, J. A. Tostevin, R. C. Johnson, and K.-I. Kubo, Nucl. Phys. **A415**, 230 (1984).
[4] H. Ohnishi, M. Tanifuji, M. Kamimura, and M. Yahiro, Phys. Lett. **118B**, 16 (1982); H. Ohnishi, M. Tanifuji, M. Kamimura, Y. Sakuragi, and M. Yahiro, Nucl. Phys. **A415**, 271 (1984).
[5] Y. Sakuragi, M. Yahiro, and M. Kamimura, Prog. Theor. Phys. **68**, 322 (1982); **70**, 1047 (1983).
[6] M. Kamimura, M. Yahiro, Y. Iseri, Y. Sakuragi, H. Kameyama, and M. Kawai, Prog. Theor. Phys. Suppl. **89**, 1 (1986), and references therein.
[7] Y. Sakuragi, M. Yahiro, and M. Kamimura, Prog. Theor. Phys. Suppl. **89**, 136 (1986), and references therein.
[8] Y. Sakuragi and Y. Hirabayashi, in *Proceedings of the Fifth International Conference on Clustering Aspects in Nuclear and Subnuclear Systems*, Kyoto, Japan, 1988, edited by K. Ikeda, K. Katori, and Y. Suzuki [J. Phys. Soc. Jpn. Suppl **58**, 560 (1989)].
[9] S. Ohkubo and M. Kamimura, Phys. Lett. **150B**, 25 (1985).
[10] B. Buck and A. A. Pilt, Nucl. Phys. **A280**, 133 (1977).
[11] T. Sakuda and F. Nemoto, Prog. Theor. Phys. **62**, 1274 (1979); **62**, 1606 (1979).
[12] G. M. Crawley and G. T. Garvey, Phys. Rev. **167**, 1070 (1968).
[13] D. Dehnhard and N. M. Hintz, Phys. Rev. C **1**, 460 (1970).
[14] T. P. Krick, N. M. Hintz, and D. Dehnhard, Nucl. Phys. **A216**, 549 (1973).
[15] R. de Swiniarski, A. Genoux-Lubain, G. Bagieu, and J. F. Cavaignac, Can. J. Phys. **52**, 2422 (1974).
[16] M. Kamimura (private communication).
[17] D. J. Pullen, J. R. Rook, and R. Middleton, Nucl. Phys. **51**, 88 (1964).
[18] R. N. Glover and A. D. W. Jones, Phys. Lett. **16**, 69 (1965).
[19] P. W. Keaton, Jr., D. D. Armstrong, L. R. Veeser, H. T. Fortune, and N. R. Roberson, Nucl. Phys. **A179**, 561 (1972).
[20] D. Fick, R. E. Brown, W. Gruebler, R. A. Hardekopf, and J. S. Hanspal, Phys. Rev. C **29**, 324 (1984).
[21] U. C. Voos, W. von Örtzen, and R. Bock, Nucl. Phys. **A135**, 207 (1969).
[22] N. Kato, K. Anai, T. Tachikawa, H. Fujita, K. Kimura, T. Sugimitsu, and Y. Nakajima, Phys. Lett. **120B**, 314 (1983).
[23] T. Wada, optical model computer code SEARCH, 1972, IPCR (unpublished).
[24] P. Charles, F. Auger, I. Badawy, B. Berthier, M. Dost, J. Gastebois, B. Fernandez, S. M. Lee, and E. Plagnol, Phys. Lett. **62B**, 289 (1984).
[25] H. H. Gutbrod, R. Bock, W. von Örtzen, and U. C. Schlotthauer-Voos, Z. Phys. **262**, 377 (1973).
[26] Y. Hirabayashi and Y. Sakuragi, Phys. Lett. B **258**, 11 (1991).
[27] Y. Hirabayashi and Y. Sakuragi, Nucl. Phys. **A536**, 375 (1992).
[28] Y. Hirabayashi, Y. Sakuragi, and M. Tanifuji, Phys. Lett. B **318**, 32 (1993).
[29] M. Kamimura (private communication).
[30] M. B. Golin and S. Kubono, Phys. Rev. C **20**, 1347 (1979).
[31] W. von Oertzen and H. G. Bohlen, Phys. Rep. **19**, 1 (1975), and references therein.
[32] R. M. DeVries, Nucl. Phys. **A212**, 207 (1973).
[33] Y. Sakuragi, Phys. Rev. C **35**, 2161 (1987).
[34] W. G. Love, T. Terasawa, and G. R. Satchler, Nucl. Phys. **A291**, 183 (1977).
[35] K.-I. Kubo and P. E. Hodgson, Nucl. Phys. **A336**, 320 (1981).
[36] T. Takemasa (private communication).
[37] T. Tamura, coupled channels computer code JUPITOR-1, Oak Ridge National Laboratory Report No. ORNL-4152, 1967.
[38] T. Tamura, Rev. Mod. Phys. **37**, 679 (1965).